RSC Advances

REVIEW

View Article Online
View Journal | View Issue

Cite this: *RSC Adv.*, 2021, **11**, 16633

Recent developments in natural mineral-based separators for lithium-ion batteries

Fangfang Liu and Xiuyun Chuan*

Lithium-ion batteries (LIBs) are currently the most widely used portable energy storage devices due to their high energy density and long lifespan. The separator plays a key role in the battery, and its function is to prevent the two electrodes of the battery from contacting, causing the internal short circuit of the battery, and ensuring the lithium ions transportation. Currently, lithium ion battery separators widely used commercially are polyolefin separators, such as polyethylene (PE) and polypropylene (PP) based separators. However, polyolefin separators would shrink at high temperatures, causing battery safety issues, and also causing white pollution. To solve these issues, the use of natural minerals to prepare composite separators for LIBs has attracted widespread attention owing to their unique nano-porous structure, excellent thermal and mechanical stability and being environmentally friendly and low cost. In this review, we present recent application progress of natural minerals in separators for LIBs, including halloysite nanotubes, attapulgite, sepiolite, montmorillonite, zeolite and diatomite. Here, we also have a brief introduction to the basic requirements and properties of the separators in LIBs. Finally, a brief summary of recent developments in natural minerals in the separators is also discussed.

Received 12th April 2021
Accepted 27th April 2021

DOI: 10.1039/d1ra02845f

rsc.li/rsc-advances

1. Introduction

LIBs are currently the most widely used portable electrochemical energy storage devices, and they are also considered the best choice for new energy vehicle power systems.[1–4] Because of their wide application characteristics and broad market prospects, LIBs have attracted a lot of attention. LIBs are mainly composed of cathodes, anodes, separator and electrolytes. As an important part of LIBs, the separator's pore structure, physical and chemical properties have a significant influence on the durability, safety and performance of the LIBs.[5,6] In a LIB, separator has the following functions: (a) separating the two electrodes to prevent internal short circuit; (b) acting as the medium for lithium ions transportation freely; (c) insulating electronic to hinder electron transmission.[7,8] A typical separator has excellent electrochemical, thermal and mechanical stability to ensure cycle stability and safety during battery operation. A hierarchical structure of the separator, with uniform pore size, should be necessary to enable Li-ion transportation and liquid electrolyte adsorption. In addition, the excellent electrolyte wettability is also required for fast Li^+ movement and low interface resistance between electrodes and electrolyte.[7,9] In lithium–sulfur (Li–S) batteries, in addition to the functions required by the separator in LIBs, the separator needs more functions, such as inhibiting the shuttle effect of polysulfides to ensure the long cycle life of Li–S batteries.[10] Utilizing the electrostatic attraction between cationic polymers and polysulfides, Li and co-workers[11] prepared CNT@cationic polymer/rGO (CNTs@CP/rGO)-functionalized separator to inhibit the shuttle effect of polysulfide, thereby ensuring the long cycle life of Li–S batteries. Liu and co-workers[12] proposed for the first time that cellulose nanocrystals (CNCs) was used as a multifunctional polysulfide stopper in Li–S batteries. On the one hand, CNCs can be used as a binder to confine sulfur and polysulfides on the cathode. On the other hand, it can limit the shuttle effect of polysulfides. These two facts work together to ensure the excellent cycle performance of Li–S batteries.

At present, polyolefin separators, such as polyethylene (PE), polypropylene (PP), are used in commercial LIBs due to their low cost, good mechanical properties, excellent chemically inert, non-toxicity, *etc.*[13] While, there are still some issues, for example, poor electrolyte wettability and thermal stability, low porosity and melting point, leading to safety issues and severely affecting electrochemical performance.[7,14] Natural minerals with abundant pore structure, excellent thermal/chemical stability and mechanical properties have attracted widespread attention. Natural minerals have unique micro- and nano-pore structures, rich resources, low cost and environmentally friendly.[15] Therefore, introducing an appropriate amount of natural minerals into the polyolefin separator of LIBs can improve the thermal shrinkage and poor mechanical strength of the polyolefin separator. Yang and co-workers[16]

Key Laboratory of Orogenis Belts and Crustal Evolution, School of Earth and Space Sciences, Peking University, Beijing 100871, China. E-mail: xychuan@pku.edu.cn

Table 1 Parameters of separators for LIBs and the typical experimental techniques, adapted from ref. 21, 30, 34 and 35

Parameter	Ideal value	Experimental calculating
Thickness (μm)	<25	Micrometer
Porosity (%)	40–60	Eqn (1)
Pore size (μm)	<1	Eqn (2)
Pore size distribution	Uniform	SEM
The degree of crystallinity	Lower	Eqn (3)
Wettability for electrolyte	High	Contact angle and eqn (4)
Dimensional stability	No curl up and lay flat (shrinkage < 5%)	Eqn (6)
Ionic conductivity (S cm^{-1})	$>10^{-4}$	Eqn (7)
Thermal stability	<5% after 1 h at 90 °C	Eqn (8)
Mechanical properties	High	Tensile test
Chemical stability	Long-term stability	

prepared an ATP (attapulgite)–PVA (polyvinylalcohol)/Celgard 2400 separator with a sandwich structure by depositing a mixture of ATP and PVA on the surface of Celgard. Compared with Celgard2400, ATP–PVA/Celgard 2400 separator exhibits outstanding mechanical properties, affinity with electrolyte and electrochemical performance. Nano-ppy/OMMT-coated separator was prepared *via* coating nano-ppy/OMMT on the surface of PE.[17] It was reported in the article that when the content of OMMT was 6%, the nano-ppy/OMMT-coated separator exhibited the highest ionic conductivity, electrolyte uptake and the most excellent electrochemical performance. Li and co-workers[18] prepared a composite separator *via* coating a mixture of diatomite and PVDF (polyvinylidene fluoride) on the surface of PET. The investigation on the influence of the mass ratio between diatomite and PVDF on the properties of the composite separator showed that the performance of the composite separator was the best when the content of diatomite was 80%. In addition to applying natural mineral-coated polyolefin separators to LIBs, Wang and co-workers[19] has prepared ISC/C@Celgard separator for Li–S batteries with excellent electrolyte affinity and mechanical stability. In view of the fact that the introduction of natural minerals can effectively improve the drawbacks of polyolefin separators in LIBs and Li–S batteries, therefore, its application in separators for LIBs and Li–S batteries has great prospects. In this review, we will give the basic requirements and properties of lithium-ion battery separators, and summarize the recent progress of natural mineral based separators for LIBs. The structure of this review includes requirements and properties of separators, application of clay minerals in LIBs separator and summary.

2. Requirements and properties of separators

Separators act an important role in the LIBs and have a huge effect on the performances of LIBs.[20] There are various techniques and requirements to characterize the performances of a separator in a LIB, such as thickness, porosity, pore size, permeability, wettability for electrolyte, dimensional stability, ionic conductivity (IC), thermal, mechanical and chemical stability. In this section, we have a detailed description of obvious parameters that characterize the properties of the separators (Table 1).

2.1 Thickness

Separator with thinner thickness has lower contact resistance while exhibiting higher energy and power density.[21] However, the thin separators will weaken the mechanical properties and safety during the battery assembly and operation.[22] Moreover, the thickness of the separators should be uniform to ensure even distribution of current during cell operation.[23]

2.2 Porosity

Separators need to show suitable porosity to keep the abundant electrolyte to allow ionic transportation and reduce internal resistance.[24] However, a separator with the excessive porosity will adversely affect safety of the battery, because it will decrease separator mechanical strength.[6] The porosity of the separator can be calculated with the eqn (1):[25]

$$\text{Porosity}(\%) = \left(1 - \frac{\rho_M}{\rho_P}\right) \times 100 \quad (1)$$

where ρ_M is the apparent density of the separator and ρ_P is the density of the polymer.

2.3 Pore size distribution

The pore size of separators is an important characteristic. The pore size should be larger than the diameter of lithium ions to allow lithium ions transportation. However, the pore size of separator is required to be smaller than the size of electrode material particles to prevent short circuits inside the battery causing by avoiding the particles and lithium metal dendrites from penetrating through the separators. In addition to the pore size, the uniformity morphology and tight pore size distribution across the separator is critically key. Non-uniform pore size distribution could lead to uneven current distribution at the interface between electrode and separator,[8] a non-uniform current distribution will promote the growth of lithium dendrites in the battery and reduce the battery performance. Pore dimension can be calculated by eqn (2):[26]

$$d = -\frac{4\gamma \cos\theta}{\Delta P} \quad (2)$$

where d is the pore diameter, ΔP is the pressure difference across the pore, γ is the surface tension of the liquid, and θ is the contact angle.

2.4 The degree of crystallinity

The higher crystallinity separator exhibits poor compatibility with electrolyte and low ionic conductivity.[27] The degree of crystallinity (X_c) can be calculated by eqn (3):[28]

$$X_c = \frac{\Delta H_m^{sample}}{\Delta H_{100}} \quad (3)$$

where ΔH_m^{sample} is the melting peak enthalpy in DSC, ΔH_{100} is the apparent melting enthalpy per gram of fully crystalline polymer.

2.5 Wettability for electrolyte

The good ion conductivity and rate capability inside battery depends upon the wettability of the electrolyte to the separator.[29] The separator should quickly adsorb the electrolyte and retain the absorbed electrolyte to achieve high ion conductivity during the charge and discharge process. The wetting speed of the separator is associated with several factors, such as its material properties and porosity[21]. The electrolyte contact angle is used to qualitatively describe the wettability of the separator. The procedure is to drop electrolyte onto the separator, and then measure the angle (θ) (Fig. 1). The smaller the θ, the better wettability of the surface separator for the electrolyte. The electrolyte uptake and retention can be calculated by eqn (4) and (5),[24] respectively.

$$\text{Electrolyte uptake}(\%) = \frac{W_{wet} - W_{dry}}{W_{dry}} \times 100 \quad (4)$$

$$\text{Electrolyte rentention}(\%) = \frac{W_{wet} - W_{dry}}{W_{wet}} \times 100 \quad (5)$$

where W_{dry} and W_{wet} are the weights of dry and electrolyte soaked separator, respectively.

2.6 Dimensional stability

Separator is required to lay flat before and after soaked electrolyte,[30] instability of the separator dimensions could cause a short circuit. Shrinkage is a parameter that characterizes dimensional stability of the separator, it is calculated by measuring the change in size of the separator in either direction during cell assembling and battery operation, as shown in eqn (6):[23]

$$\text{Dimensional shrinkage}(\%) = \frac{L_b - L_a}{L_b} \times 100 \quad (6)$$

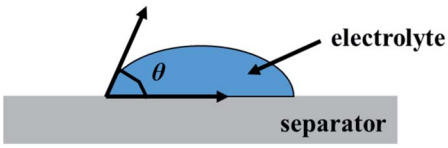

Fig. 1 The electrolyte contact angle.

where L_b and L_a are the sizes of the separator in either direction before and after soaked electrolyte or battery operating, respectively.

2.7 Ionic conductivity (IC)

The IC of separators is a key norm. The high IC will achieve excellent battery capacity, rate performance, cycle life and lower cell resistance.[31] The IC of separators is affected by the porosity and transportation performance of the electrolyte ions absorbed in the separator. And ions homogeneous transportation is crucial for battery cycling stability.[32] The IC value can be determined by electrochemical impedance spectroscopy (EIS) on the electrolyte-soaked separator. The IC is evaluated by the following eqn (7):[24]

$$\sigma = \frac{l}{R_b A} \quad (7)$$

where σ is the IC, l and A are the thickness and area of separator, respectively, R_b is the bulk resistance.

2.8 Thermal stability

The thermal stability of a separator is important to safety of the battery. Thermal shrinkage of the separator will cause to short circuit. The thermal shrinkage of separators can be estimated by eqn (8):[33]

$$\text{Thermal shrinkage}(\%) = \frac{D_b - D_a}{D_b} \times 100 \quad (8)$$

where D_b and D_a are the areas of the separator before and after heating, respectively.

2.9 Mechanical properties

The sufficient mechanical strength of the separator is crucial for battery assembly and operation. During cell operating, the separator is subject to mechanical deformation caused by external compression or electrode materials volume expansion.[23] In addition, the separator is required to inhibit piercing of lithium dendrites to avoid the internal short circuit. The mechanical strength of the separator is negatively related to its porosity, which means that the higher the porosity of the separator, the lower its mechanical strength. Therefore, it is necessary to find a balance between porosity and mechanical strength to obtain excellent electrochemical performances.

2.10 Chemical stability

In order to obtain long lifespan battery, the separator should show excellent chemical stability to prevent degradation and reduction of mechanical properties caused by reaction or dissolution with the electrolyte.[21,22] The separator should not react with the electrolyte and electrode materials. Moreover, the strong oxidizing and reducing environment generated by the electrode material during the operating process of the battery, the separator must be electrochemically stable to achieve long life of cell.[6]

2.11 Electrochemical stability

In addition to the structural physical and chemical properties mentioned above, the electrochemical properties of the separator must also be tested by linear sweep voltammetry (LSV) and cycling with Li metal (reference and counter electrodes)/the tested separator/stainless-steel (working electrode).[31]

3. Application of natural minerals in LIBs separator

Natural minerals can be widely obtained from nature, with abundant reserves, low price and environmentally friendly, in line with the requirements of environmental protection and

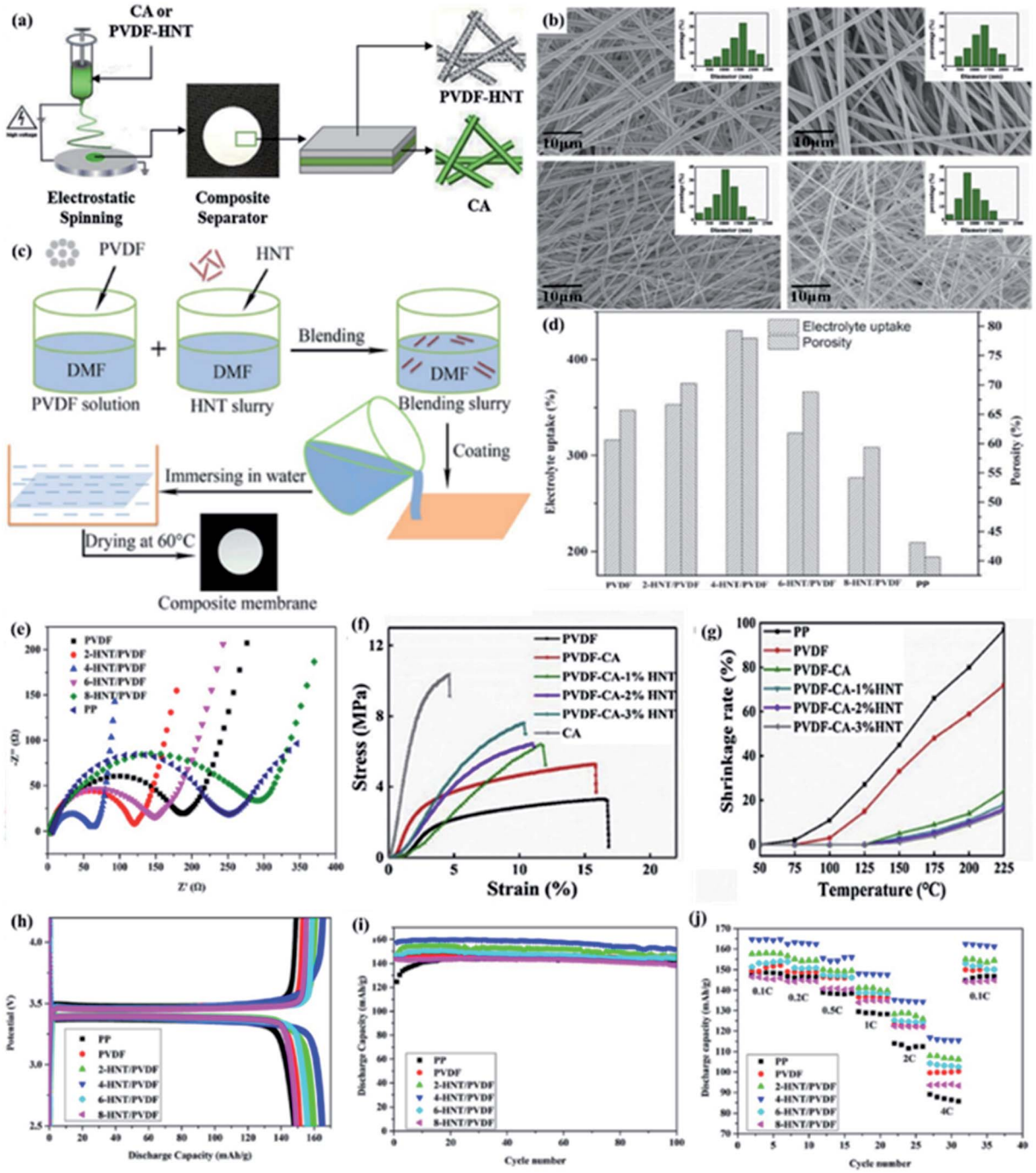

Fig. 2 (a) Preparation procedure of the PVDF-CA-HNT composite separators, (b) surface morphology SEM image and their fiber diameter size distribution of composite separators, reprinted from ref. 37 with permission from Copyright© 2019 Elsevier. (c) Schematic illustration for the experimental procedure of the HNT/PVDF composite separators, (d) electrolyte uptake and porosity and (e) EIS of composite separators, reprinted from ref. 38 with permission from Copyright© 2019 Elsevier B.V. (f) Stretching curves and (g) thermal shrinkage properties of various separators, reprinted from ref. 37 with permission from Copyright© 2019 Elsevier. (h) Initial charge–discharge profiles at 0.1C, (i) cycling performance at 0.5C and (j) rate performance. Reprinted from ref. 38. with permission from Copyright© 2019 Elsevier B.V.

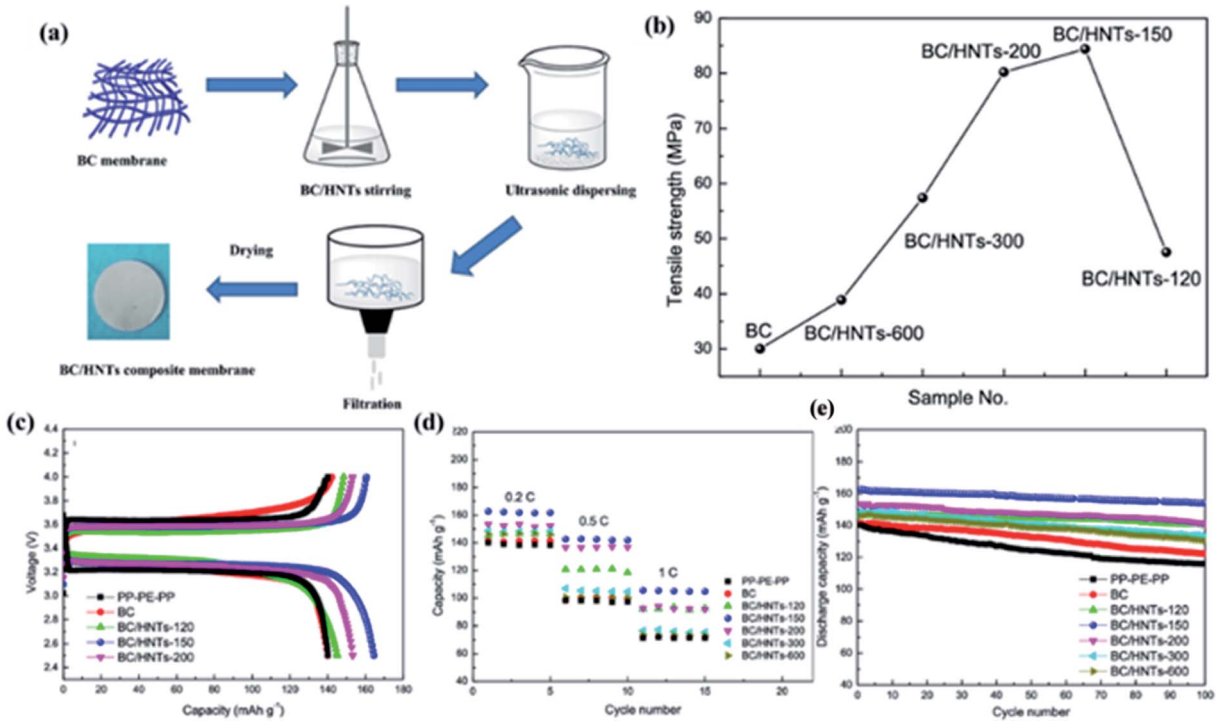

Fig. 3 (a) Schematic illustration of the membrane preparation procedure, (b) tensile strength of the BC/HNTs separators, (c) charge/discharge profiles, (d) rate capability and (e) cycling performance of the batteries with the PP–PE–PP, BC and BC/HNTs separators. Reprinted from ref. 36 with permission from Copyright© 2020 Springer Nature Switzerland AG. Part of Springer Nature.

sustainable development. Recently, the application of natural minerals to lithium-ion battery separators has fascinated focus because of the large amount of properties of natural minerals, such as excellent mechanical properties, abundant pore structure, good electrolyte wettability and high thermal stability. The various clay minerals widely used in lithium-ion battery separators mainly include halloysite,[36–38] attapulgite,[16,39] sepiolite,[40] montmorillonite[17,41–44] and zeolite.[45–48] The types of clay mineral composite LIB separators can be divided into one-dimensional clay mineral based composite separators, two-dimensional clay mineral based composite separators and three-dimensional clay minerals composite separators

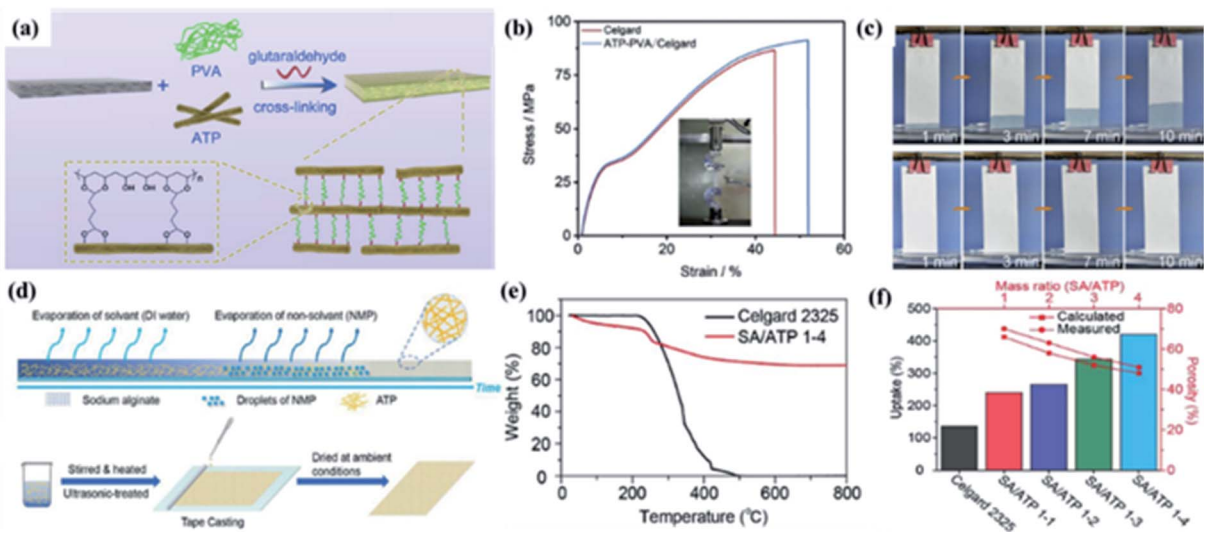

Fig. 4 (a) Schematic illustration for the ATP–PVA/Celgard separator preparation. (b) Tensile stress–strain curves and (c) climbing behaviors of electrolyte of the separators. Reprinted from ref. 16 with permission from Copyright© 2020 Elsevier. (d) Schematic illustration of the overall procedure of the SA/ATP 1-4 separator preparation, (e) TGA curves and (f) electrolyte uptake and porosity of separators. Reprinted from ref. 39 with permission from Copyright© 2019 Elsevier B.V.

according to the dimensions of clay minerals used in the separator. In the following sections, we will introduce these three composite separators one by one.

3.1 One-dimensional(1D) minerals

3.1.1 Halloysite (HNT). Halloysite (idealized half unit cell formula-$Al_2(OH)_4Si_2O_5 \cdot 2H_2O$) is a two-layered aluminosilicate mineral, including one alumina octahedron sheet and one silica tetrahedron sheet in 1 : 1 stoichiometric ratio,[49] it is similar to kaolinite but possesses an additional water monolayer between the 1 : 1 aluminosilicate layers and an unique tubular structure,[50] and the tubular structure is caused by the halloysite layer wrapping. Recently, due to the hollow tubular structure, considerable aspect ratio, excellent tensile strength, the presence of hydroxyl groups on the surface, high thermal stability, low cost and environmental friendliness of halloysites,[38] HNTs have attracted wide attention for its application in separators. Considering the above characteristics, HNTs are applied to high-performance LIB separators.

Wang *et al.* prepared a sandwich-structured PVDF-CA-3% HNT composite separator *via* electrospinning technique (Fig. 2a), which had higher porosity, mechanical properties, thermal dimensional stability and ionic conductivity.[37] Xu at al prepared the HNT/PVDF separator *via* vacuum filtration (Fig. 2c), with higher IC and excellent electrochemical performance.[38] As shown in Fig. 2b, there are straight and staggered fibers, and HNT with hollow tubular structure could provide channels for lithium ions to improve the lithium ions transportation efficiency. Moreover, the higher porosity and the hydrogen bonding on the surface of HNT contributes to higher electrolyte uptake (Fig. 2d) in favor of higher IC and lower interfacial resistance between electrodes and separators (Fig. 2e). As shown in Fig. 2f and g, the addition of HNT, the tensile strength of the separator increased from 5.3 MPa (PVDF-CA) to 7.6 MPa (PVDF-CA-3%HNT separator), the thermal shrinkage of the separator decreased from 24% (PVDF-CA) to 15% (PVDF-CA-3%HNT separator) at 225 °C, respectively. Separator with excellent mechanical properties and thermal stability is of vital importance to battery safety. The Lewis acid site on the surface of HNT can inhibit the decomposition of anions by interacting with PF_6^- in the electrolyte,[51] and the tubular structure of HNT can store the electrolyte to prevent the oxidation of the electrolyte.[52] These two factors together improve the electrochemical stability of the separator. Compared with the separators without HNT, the composite separator with the addition of HNT has higher porosity, IC, electrochemical stability, and lower interfacial impedance, and represents excellent electrochemical performances (Fig. 2h–j).

Huang *et al.* used bacterial cellulose (BC) and halloysite nanotubes (HNTs) as raw materials to prepare a BC/HNTs nanofiber composite separator by vacuum filtration (Fig. 3a).[36] Due to the existence of hydrogen bonding, there are strong interactions between HNT and BC, and HNTs exhibit enhanced functions, so that the mechanical strength of the BC/HNTs composite separators is significantly improved, as shown in Fig. 3b. Good mechanical performance of separator is an important parameter to ensure battery safety. Due to the addition of HNTs, the porosity, electrolyte uptake, and permeability of the BC/HNTs separator are significantly improved. These factors all promote the ion migration, thus contributing to the high capacity (Fig. 3c), rate performance (Fig. 3d) and long cycle life (Fig. 3e) of LIBs.

3.1.2 Attapulgite(ATP). Attapulgite (idealized half unit cell formula-$Si_8Mg_8O_{20}(OH)_2(H_2O)_4 \cdot 4H_2O$), also known as palygorskite, is a kind of water-containing magnesium-rich aluminum silicate mineral with a 2 : 1 chain layered structure.[53,54] ATP shows excellent thermal,[55] mechanical[56] stability, high aspect ratio, abundant micro–nano-sized channels[16] and many silanol groups on its surface.[54] These physico-chemical characters make it receive greater attention in the LIB separator area.

Yang and coworkers fabricated ATP–PVA/Celgard separator with a sandwiching structure *via* the simple dip-coating method (Fig. 4a).[16] As shown in Fig. 4b, the ATP–PVA/Celgard composite

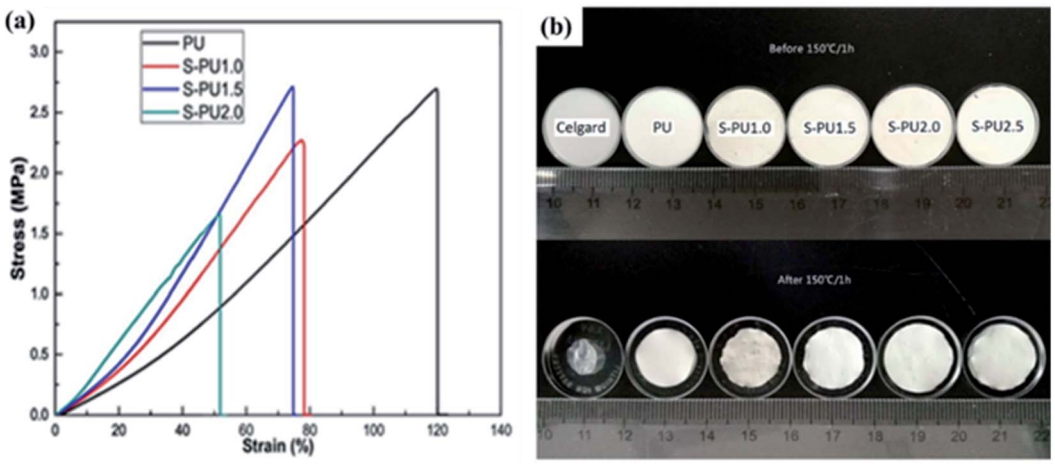

Fig. 5 (a) Stress–strain curves and (b) digital pictures (heated by 150 °C for 1 h) of the separators. Reprinted from ref. 34 with permission from Copyright© 2019 Elsevier B.V.

separator showed higher tensile strength, which is mainly due to the ATP–PVA suspension with excellent mechanical stability deposited onto Celgard separator and the formation of a sandwiching/infusing structure, which could improve the safety of LIBs. The ATP–PVA/Celgard separator showed good electrolyte wettability and higher electrolyte uptake (Fig. 4c), which enhanced Li^+ conductivity and cycling stability of LIBs. Furthermore, Song and coworkers prepared a naturally degradable, thermally stable, and eco-friendly SA/ATP 1-4 separator fabricated with attapulgite (ATP) nanofibers and sodium alginate (SA) by a facile phase inversion process (Fig. 4d).[39] The SA/ATP 1-4 separator exhibited good thermal stability because of the high thermal stability of ATP (Fig. 4e), which is essential to the safety of LIBs. In addition, SA/ATP composite separators had higher porosity and electrolyte uptake than Celgard 2325 (Fig. 4f), which ensures the migration of lithium ions, and were of great significance to the improvement electrochemical performance.

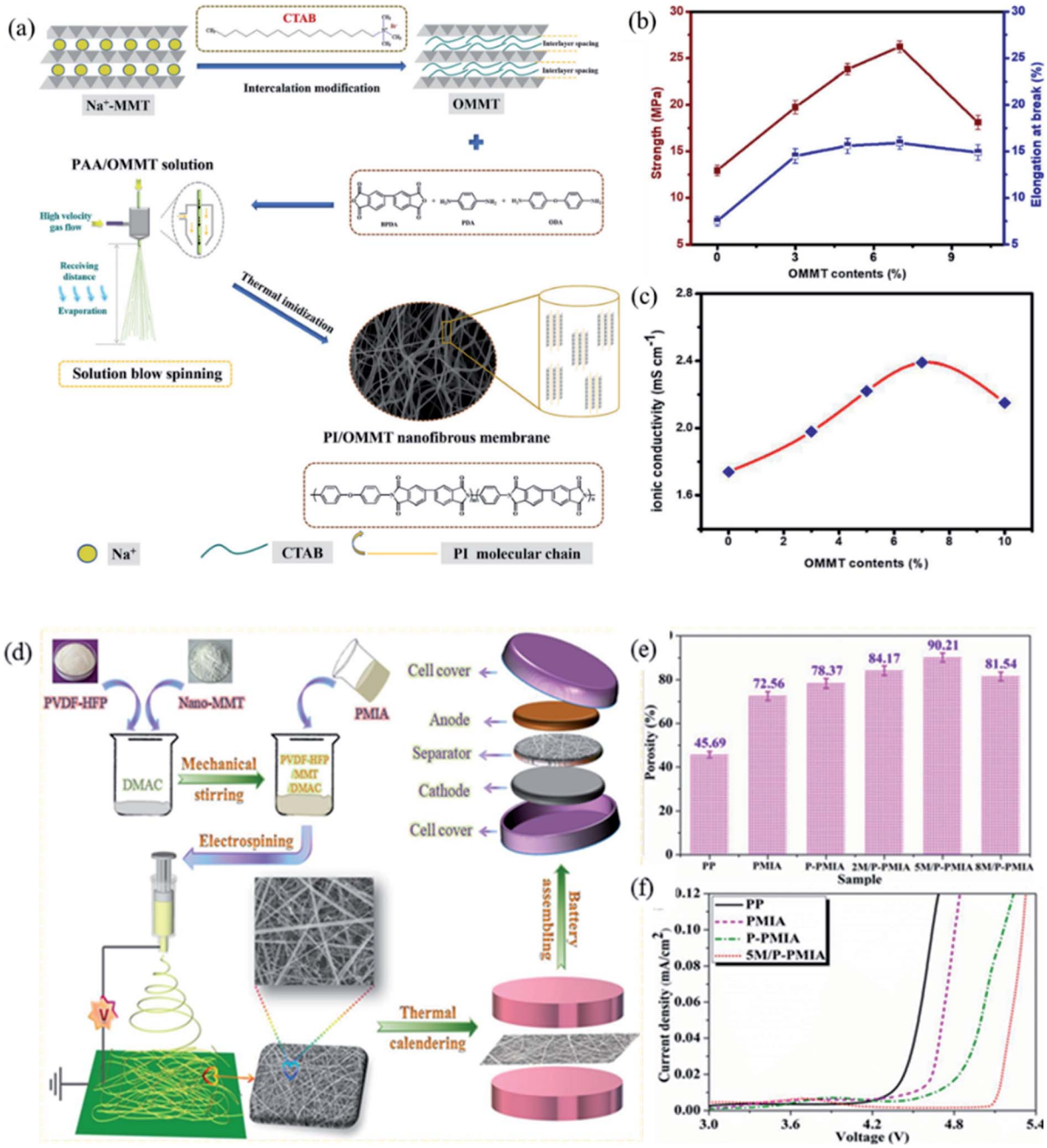

Fig. 6 (a) Schematic illustration of Na-MMT intercalation modification and (b) PI/OMMT nanofibrous membrane preparation, (c) variation of mechanical properties and ionic conductivity of PI/OMMT hybrid separators, reprinted from ref. 63 with permission from Copyright© 2020 American Chemical Society. (d) The schematic illustration of M/P-PMIA separator preparation and battery reassembly, (e) the porosity and (f) electrochemical window plots of separators. Reprinted from ref. 41 with permission from Copyright© 2019 Elsevier B.V.

3.1.3 Sepiolite. Sepiolite (ideal chemical formula-$Mg_8Si_{12}O_{30}(OH)_4(H_2O)_4\cdot 4H_2O$) is a water-containing magnesium silicate clay mineral with 2 : 1 tri-octahedral sheet.[57] Sepiolite is widely used in the fields of adsorption,[58] catalysis[59] and so on. Nowadays, because of the fibrous micromorphology, high porosity and specific surface area, excellent mechanical and thermal stability of sepiolite, its application in the field of energy storage has attracted wide attention, such as battery electrode materials[60] and separators.[40]

Deng and coworkers fabricated sepiolite-based battery separators (S-PU1.5) by electrospinning method.[40] As shown in Fig. 5a, the elastic modulus of the S-PU composite separator is positively correlated with the sepiolite content, which may be related to the fibrous micromorphology of sepiolite. From the digital picture (Fig. 5b), we can obviously see that S-PU composite separators exhibit excellent thermal stability, while the Celgard shows significant shrinkage. Both excellent mechanical and thermal stability can ensure the safety of the battery during operation.

3.2 Two-dimensional(2D) minerals

3.2.1 Montmorillonite (MMT). Montmorillonite (idealized half unit cell formula-$(Na, Ca)_{0.33}(Al, Mg)_2[Si_4O_{10}](OH)_2\cdot nH_2O$) is a typical 2 : 1 aluminosilicate layered clay mineral. Montmorillonite has many special features including excellent thermal and mechanical stability, layered nanostructure, high aspect ratio, and high intercalation/exfoliation capacity.[61] Due to its high ion exchange capacity, the silicon and aluminum ions in the middle layer are easily replaced by other cations, which will make the layer appear electronegative. At the same time, the cations between the montmorillonite layers will interact with lithium ions, which improves the ionic conductivity.[62] In addition, hydrophilic montmorillonite can improve the wettability of liquid electrolytes and promote Li^+ movement.[41] In view of the above characteristics, recently, as a member of the clay mineral family, montmorillonite as a nano-filler in lithium ion battery separators has attracted widespread attention from many researchers.

The hydrophobic functional groups on the surface of the PE separator result in poor compatibility with organic electrolytes, thus increasing the interface resistance of the battery. In addition, the PE separator will thermal shrink at elevated temperature, which will result in a short circuit of the battery and cause a safety accident. To enhance the thermal stability of the PE separator, Yang and coworkers prepared nanopolypyrrole/organic montmorillonite-(ppy/OMMT-) coated separator by coating ppy/OMMT with excellent thermal stability onto the PE.[17] Compared with PE separator, ppy/OMMT-coated separator had a higher decomposition temperature, which greatly improved the thermal stability of the separator. Considering that polyolefin separator will cause white pollution, Li and coworkers fabricated PI/OMMT separator *via* the solution blow spinning method for the first time (Fig. 6a).[63] Compared with Celgard 2400 and PI separator, montmorillonite as a nano-filler can obviously promote the mechanical properties of the PI/OMMT separator (Fig. 6b), the montmorillonite filler uniformly dispersed in the polyimide polymer matrix makes the separator both rigid and flexible. The nanosilicate layer in the montmorillonite has a good affinity with the electrolyte, which improves the hydrophilicity of the separator, thereby ensuring the good wettability of the separator to electrolyte. Higher electrolyte uptake and superior electrolyte affinity reduced the migration resistance of Li^+ between the electrodes and separator, showing high ionic conductivity (Fig. 6c). Fang and coworkers fabricated PVDF-based composite separator with different contents of montmorillonite (MMT) *via* electrospinning.[42] Further improve the electrolyte uptake, mechanical

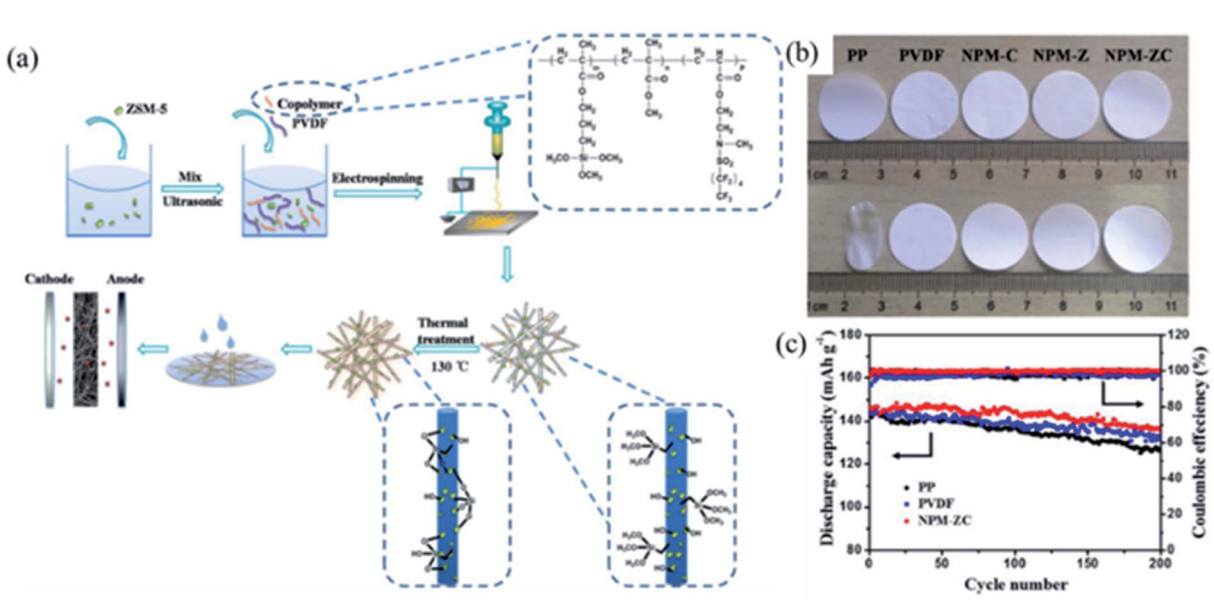

Fig. 7 (a) Schematic illustration of the preparation procedure for separators, (b) photographs of separators (heated by at 150 °C for 1 h), (c) cycling stability at 0.2C, reprinted from ref. 47 with permission from Copyright© 2018 Elsevier B.V.

Table 2 Performance of the composite separators mentioned above for LIBs

Separator	Method	Electrode materials	Liquid electrolyte	Thickness (μm)	Crystallinity (%)	Porosity (%)	Electrolyte uptake (%)	Tensile strength (MPa)	Thermal dimensional stability (shrinkage %)	Ionic conductivity (mS cm^{-1})	Cycling stability: retention, cycles	Electrochemical performance: specific capacity (mA h g^{-1}), rate (C)	Ref.
PVDF-CA	Electrospinning	Li/$LiCoO_2$	$LiPF_6$	30	25.8	87.6	177	5.3	24% (225 °C)	1.02	87.07%, 50	142.05, 0.2C	37
PVDF-CA-3% HNT	Electrospinning	Li/$LiCoO_2$	$LiPF_6$	30	20.2	86.3	311	7.6	15% (225 °C)	1.36	91.8%, 50	145.6, 0.2C	37
BC	Vacuum filtration	Li/$LiFePO_4$	$LiPF_6$–EC/DMC/DEC	30	—	73.7	284	30	Closed to 0% (180 °C, 0.5 h)	2.88	86%, 100	141, 0.2C	36
BC/HNTs-150	Vacuum filtration	Li/$LiFePO_4$	$LiPF_6$–EC/DMC/DEC	30	—	83.0	369	84.4	Closed to 0% (180 °C, 0.5 h)	5.13	95%, 100	162, 0.2C	36
PVDF	Phase inversion	Li/$LiFePO_4$	$LiPF_6$–EC/DMC	—	16.45	Closed to 66	Closed to 320	—	Severe curl (150 °C, 0.5 h)	1.33	84.42%, 100	151.28, 0.1C	38
4-HNT/PVDF	Phase inversion	Li/$LiFePO_4$	$LiPF_6$–EC/DMC	—	12.73	Closed to 77.5	430.2	—	Slightly curl (150 °C, 0.5 h)	2.40	89.12%, 100	164.72, 0.1C	38
Celgard	Deposition	Li/$LiNi_{0.5}Mn_{1.5}O_4$ Li/$LiFePO_4$	$LiPF_6$–EC/DMC	25	—	44.1	89.3	—	Slightly shrinkage (170 °C, 0.5 h)	0.537	Decayed rapidly, 70	—	16
ATPPVA/Celgard	Deposition	Li/$LiNi_{0.5}Mn_{1.5}O_4$ Li/$LiFePO_4$	$LiPF_6$–EC/DMC	28.3 ± 0.6	—	45.8	168.2	Enhance 5.54%	No obvious shrinkage (170 °C, 0.5 h)	0.782	91.7%, 200	—	16
Celgard 2325	Phase inversion	Li/$LiFePO_4$	$LiPF_6$–EC/DEC	—	—	—	130	—	Burned away (250 °C, 2 h)	0.95	68.7%, 700	148.9, 0.5C	39
SA/ATP 1-4	Phase inversion	Li/$LiFePO_4$	$LiPF_6$–EC/DEC	20	—	—	420	6	Remained intact (250 °C, 2 h)	1.15	82.2%, 700	152, 0.5C	39
PP	—	Li/$LiFePO_4$	$LiPF_6$–EC/DEC/DMC	25	—	44	72	—	78% (150 °C, 1 h)	0.35	—	—	40
S-PU1.5	Electrospinning	Li/$LiFePO_4$	$LiPF_6$–EC/DEC/DMC	81	—	64	268	—	No obvious shrinkage (150 °C, 1 h)	1.37	—	150, 0.2C,	40
PE	—	Li/$LiNi_{1/3}Co_{1/3}Mn_{1/3}O_2$	$LiPF_6$–EC/DEC/EMC	10	—	—	146	1.24	8% (80 °C, 5 h)	1.95	60%, 100	123.7, 0.5C	17
OMMT-coated PE	Coating	Li/$LiNi_{1/3}Co_{1/3}Mn_{1/3}O_2$	$LiPF_6$–EC/DEC/EMC	—	—	—	349	3.39	No significant shrinkage (80 °C, 5 h)	4.31	80%, 100	125.9, 0.5C	17
Celgard 2400	—	Li/$LiCoO_2$	$LiPF_6$–EC/DEC/EMC	25	—	41.5	125	—	79% (180 °C, 0.5 h)	Lower than PI/7 wt% OMMT	73.4%, 100	—	63
PI	Solution blow spin-ing	Li/$LiCoO_2$	$LiPF_6$–EC/DEC/EMC	24	—	83	450	12.95	Closed to 0% (180 °C, 0.5 h)	Lower than PI/7 wt% OMMT	84.7%, 100	—	63
PI/7 wt% OMMT	Solution blow spinning	Li/$LiCoO_2$	$LiPF_6$–EC/DEC/EMC	24	—	80	475	26.23	Closed to 0% (180 °C, 0.5 h)	2.39	86.6%, 100	135.3, 0.5C	63
P-PMIA	Electrospinning	Li/$LiCoO_2$	$LiPF_6$–EC/EMC/DEC	45	—	78.37	898	20.36	Closed to 0% (220 °C)	1.13	—	—	41
5M/P-PMIA	Electrospinning	Li/$LiCoO_2$	$LiPF_6$–EC/EMC/DEC	47	—	90.21	1027	25.59	Closed to 0% (220 °C)	2.41	88%, 200	161.2, 0.5C	41

Table 2 (*Contd.*)

Separator	Method	Electrode materials	Liquid electrolyte	Thickness (μm)	Crystallinity (%)	Porosity (%)	Electrolyte uptake (%)	Tensile strength (MPa)	Thermal dimensional stability (shrinkage %)	Ionic conductivity (mS cm^{-1})	Cycling stability: retention, cycles	Electrochemical performance: specific capacity (mA h g^{-1}), rate (C)	Ref.
PVDF	Electrospinning	Li/LiFePO$_4$	LiPF$_6$–EC/EMC/DEC	45	39.35	79.27	307	1.42	27% (150 °C, 1 h)	2.04	—	—	42
PVDF/MMT-5%	Electrospinning	Li/LiFePO$_4$	LiPF$_6$–EC/EMC/DEC	58	41.16	84.08	333	2.39	14.6% (150 °C, 1 h)	4.2	100%, 50	144, 0.2C	42
PVDF	Electrospinning	Li/LiFePO$_4$	LiPF$_6$–EC/EMC/DEC	—	42.9	73	301	2.8	Closed to 0% (150 °C, 1 h)	1.07	91.6%, 200	148, 0.1C	47
NPM-ZC	Electrospinning	Li/LiFePO$_4$	LiPF$_6$–EC/EMC/DEC	—	35.8	80	378	3.2	Closed to 0% (150 °C, 1 h)	1.72	93.8%, 200	152, 0.1C	47
PP	Coating	Li/LiFePO$_4$	LiPF$_6$–EC/DEC	25	—	40.6	—	—	39.6% (160 °C, 0.5 h)	0.19	98.09%, 100	138.8, 0.5C	18
DP-80	Coating	Li/LiFePO$_4$	LiPF$_6$–EC/DEC	118	—	63.8	—	—	1.17% (160 °C, 0.5 h)	1.43	98.26%, 100	144.3, 0.5C	18

properties and thermal stability of the composite separator, Zhao and coworkers prepared a hierarchical-structure M/P-PMIA separator containing poly(vinylidene fluoridehexafluoropropylene) (PVDF-HFP) and MMT by electrospinning method (Fig. 6d).[41] The M/P-PMIA separator had a higher porosity, which can absorb more liquid electrolytes, so as to favor the migration of Li^+ and improve the ion conductivity (Fig. 6e). Firstly, due to the presence of the anionic Lewis acid sites onto the MMT, the decomposition of electrolyte lithium salt can be inhibited. In addition, the introduction of MMT can improve the wettability of the separator to the electrolyte. These factors together improved the wettability of the separator to the electrolyte, and also promoted the excellent electrochemical stability of the M/P-PMIA separator (Fig. 6f).

3.3 Three-dimensional(3D) minerals

3.3.1 Zeolite. The structural formula of zeolite is $A_{(x/q)}[(AlO_2)_x(SiO_2)_y]\cdot n(H_2O)$. Zeolite is a kind of hydrous aluminosilicate mineral.[64] Zeolite has ion exchange capacity and unique nanoporous structure due to its many pores and channels, which has attracted wide attention in the fields of adsorption,[65,66] catalysis,[67] energy storage,[46,47] *etc.*

Considering the ion exchange characteristics of zeolite, Xu and coworkers prepared a multifunctional lithium-ion-exchanged zeolite-coated separator to solve the problem that the manganese-based electrode material is deposited on the negative electrode after being dissolved in the electrolyte, which causes the battery capacity decay.[46] Zhang and coworkers prepared a polymers/zeolite nanocomposite separator *via* electrospinning technology and thermal cross-linking method (Fig. 7a). Compared with PP separator, NPM-ZC nanocomposite separator exhibited excellent thermal stability, it was heat treated at 150 °C for 1 h without significant shrinkage (Fig. 7b). In addition to excellent thermal stability, NPM-ZC nanocomposite separator had higher electrolyte absorption, ionic conductivity, and better cycling performance (Fig. 7c).

3.3.2 Diatomite. Diatomite is a kind of biogenic siliceous sedimentary rock with highly porous structure.[68] Its chemical composition is mainly SiO_2. Its microporous structure and active silica components make diatomite widely used in the fields of adsorption,[69] purification,[70] thermal insulation,[71] sound absorption,[72] filtration[73] and energy storage.[18,74]

Li and co-workers prepared a composite separator *via* coating diatomite/PVDF mixture on the PET nonwoven.[18] The separator coated with diatomite of high temperature resistance shows excellent thermal stability. When heated at 150 °C for 1 hour, the composite separator had no significant shrinkage, thus ensuring the safe operation of LIBs at high temperatures.

4. Summary

The separator is the crucial part of the LIB. It plays an essential role in safety and cost-effective of LIBs. The separator should have a suitable pore structure to achieve a balance between high liquid absorption and mechanical stability. The thermal and chemical/electrochemical stability of the separator is also

needed to ensure the safety and durability of the battery. The recent advances in natural minerals utilized in LIBs separators are summarized in this review (Table 2). Up to now, a number of natural minerals based separators with hierarchical structure and various components have been developed *via* coating, electrospinning, vacuum filtration, solution blow spinning, phase inversion, deposition. Some advantages of minerals based separators include: (a) possessed higher thermal stability that enable safety of battery, compared with separators without natural minerals; (b) enhanced mechanical property to ensure safety during battery assembly and inhibit the growth of lithium dendrites; (c) improved affinity with electrolytes for low interface resistance; (d) porosity and electrolyte uptake were also improved because of unique and abundant nano-porous structure of natural minerals, which is beneficial for rapid ion transportation; and (e) environmentally friendly and low cost. The separator that have been reported so far usually have two or three above-mentioned merits. However, an ideal separator needs to meet all these features to achieve the high performance and durability of the battery. Therefore, it is necessary to further develop high-performance lithium-ion battery separators.

Conflicts of interest

The authors declare no conflict of interest.

Acknowledgements

The authors would like to acknowledge the support from National Natural Science Foundation of China (No. 51774016 and 52074015) and Test Fund of Peking University (0000012321).

References

1 P. Guan, L. Zhou, Z. Yu, Y. Sun, Y. Liu, F. Wu, Y. Jiang and D. Chu, *J. Energy Chem.*, 2020, **43**, 220–235.
2 A. Manthiram, *Nat. Commun.*, 2020, **11**, 1550.
3 M. Li, T. Liu, X. Bi, Z. Chen, K. Amine, C. Zhong and J. Lu, *Chem. Soc. Rev.*, 2020, **49**, 1688–1705.
4 F. Wu, J. Maier and Y. Yu, *Chem. Soc. Rev.*, 2020, **49**, 1569–1614.
5 J. Wen, Y. Yu and C. Chen, *Mater. Express*, 2012, **2**, 197–212.
6 H. Lee, M. Yanilmaz, O. Toprakci, K. Fu and X. Zhang, *Energy Environ. Sci.*, 2014, **7**, 3857–3886.
7 Y. Xiang, J. Li, J. Lei, D. Liu, Z. Xie, D. Qu, K. Li, T. Deng and H. Tang, *ChemSusChem*, 2016, **9**, 3023–3039.
8 V. Deimede and C. Elmasides, *Energy Technol.*, 2015, **3**, 453–468.
9 H. Li, D. Wu, J. Wu, L. Y. Dong, Y. J. Zhu and X. Hu, *Adv. Mater.*, 2017, **29**, 1703548.
10 P. Jovanović, M. S. Mirshekarloo, M. R. Hill, A. F. Hollenkamp, M. Majumder and M. Shaibani, *Advanced Materials Technologies*, 2021.
11 Z. Li, S. Jiao, D. Yu, Q. Zhang, K. Liu, J. Han, Z. Guo, J. Liu and L. Wang, *ACS Appl. Energy Mater.*, 2021, **4**, 2914–2921.
12 J. Liu, Y. Li, Y. Xuan, L. Zhou, D. Wang, Z. Li, H. Lin, S. Tretiak, H. Wang, L. Wang, Z. Guo and S. Zhang, *ACS Appl. Mater. Interfaces*, 2020, **12**, 17592–17601.
13 E. Rao, B. McVerry, A. Borenstein, M. Anderson, R. S. Jordan and R. B. Kaner, *ACS Appl. Energy Mater.*, 2018, **1**, 3292–3300.
14 X. Huang, *J. Power Sources*, 2014, **256**, 96–101.
15 李爱军; 传秀云; 曦, 曹.; 黄杜斌 和 苏双青, *功能材料*, , 2017, **48**, 02063–02070
16 Y. Yang, W. Wang and J. Zhang, *Mater. Today Energy*, 2020, **16**, 100420.
17 S. Yang, H. Qin, X. Li, H. Li and P. Yao, *J. Nanomater.*, 2017, **2017**, 1–10.
18 D. Li, H. Xu, Y. Liu, Y. Jiang, F. Li and B. Xue, *Ionics*, 2019, **25**, 5341–5351.
19 W. Wang, Y. Yang, H. Luo, S. Li and J. Zhang, *J. Colloid Interface Sci.*, 2020, **576**, 404–411.
20 J. C. Barbosa, J. P. Dias, S. Lanceros-Mendez and C. M. Costa, *Membranes*, 2018, **8**, 45.
21 P. Arora and Z. J. Zhang, *Chem. Rev.*, 2004, **104**, 4419–4462.
22 S. S. Zhang, *J. Power Sources*, 2007, **164**, 351–364.
23 C. F. J. Francis, I. L. Kyratzis and A. S. Best, *Adv. Mater.*, 2020, e1904205.
24 M. Waqas, S. Ali, C. Feng, D. Chen, J. Han and W. He, *Small*, 2019, **15**, e1901689.
25 K. M. Abraham, *Electrochim. Acta*, 1993, **38**, 1233–1248.
26 W. PiaÎtkiewicz, S. RosinÂski, D. LewinÂska, J. Bukowski and W. Judycki, *J. Membr. Sci.*, 1999, **153**, 91–102.
27 C. M. Costa, Y.-H. Lee, J.-H. Kim, S.-Y. Lee and S. Lanceros-Méndez, *Energy Storage Mater.*, 2019, **22**, 346–375.
28 S. W. Choi, S. M. Jo, W. S. Lee and Y. R. Kim, *Adv. Mater.*, 2003, **15**, 2027–2032.
29 B. Scrosati and J. Garche, *J. Power Sources*, 2010, **195**, 2419–2430.
30 C. M. Costa, M. M. Silva and S. Lanceros-Méndez, *RSC Adv.*, 2013, **3**, 11404–11417.
31 Y. Li, Q. Li and Z. Tan, *J. Power Sources*, 2019, **443**, 227262.
32 M. F. Lagadec, R. Zahn and V. Wood, *Nat. Energy*, 2018, **4**, 16–25.
33 M. Waqas, C. Tan, W. Lv, S. Ali, B. Boateng, W. Chen, Z. Wei, C. Feng, J. Ahmed, J. B. Goodenough and W. He, *ChemElectroChem*, 2018, **5**, 2722–2728.
34 X. Huang, *J. Solid State Electrochem.*, 2010, **15**, 649–662.
35 J. Nunes-Pereira, C. M. Costa and S. Lanceros-Méndez, *J. Power Sources*, 2015, **281**, 378–398.
36 C. Huang, H. Ji, B. Guo, L. Luo, W. Xu, J. Li and J. Xu, *Cellulose*, 2019, **26**, 6669–6681.
37 S. Wang, D. Zhang, Z. Shao and S. Liu, *Carbohydr. Polym.*, 2019, **214**, 328–336.
38 H. Xu, D. Li, Y. Liu, Y. Jiang, F. Li and B. Xue, *J. Alloys Compd.*, 2019, **790**, 305–315.
39 Q. Song, A. Li, L. Shi, C. Qian, T. G. Feric, Y. Fu, H. Zhang, Z. Li, P. Wang, Z. Li, H. Zhai, X. Wang, M. Dontigny, K. Zaghib, A.-H. Park, K. Myers, X. Chuan and Y. Yang, *Energy Storage Mater.*, 2019, **22**, 48–56.
40 C. Deng, Y. Jiang, Z. Fan, S. Zhao, D. Ouyang, J. Tan, P. Zhang and Y. Ding, *Appl. Surf. Sci.*, 2019, **484**, 446–452.
41 H. Zhao, W. Kang, N. Deng, M. Liu and B. Cheng, *Chem. Eng. J.*, 2020, 384.

42 C. Fang, S. Yang, X. Zhao, P. Du and J. Xiong, *Mater. Res. Bull.*, 2016, **79**, 1–7.
43 M. Raja, T. P. Kumar, G. Sanjeev, L. Zolin, C. Gerbaldi and A. M. Stephan, *Ionics*, 2014, **20**, 943–948.
44 J. Nunes-Pereira, A. C. Lopes, C. M. Costa, R. Leones, M. M. Silva and S. Lanceros-Méndez, *Electroanalysis*, 2012, **24**, 2147–2156.
45 W. Zeng, B. Li, H. Li, W. Li, H. Jin and Y. Li, *Sep. Purif. Technol.*, 2019, **228**, 115741.
46 J. Xu, X. Xiao, S. Zeng, M. Cai and M. W. Verbrugge, *ACS Appl. Energy Mater.*, 2018, **1**, 7237–7243.
47 J. Zhang, Y. Xiang, M. I. Jamil, J. Lu, Q. Zhang, X. Zhan and F. Chen, *J. Membr. Sci.*, 2018, **564**, 753–761.
48 张红涛; 华, 尚.; 波, 顾. and 张恒源, *材料工程*, 2017, **45**, 83–87
49 R. Zhai, B. Zhang, L. Liu, Y. Xie, H. Zhang and J. Liu, *Catal. Commun.*, 2010, **12**, 259–263.
50 B. Zhang, H. Guo, P. Yuan, L. Deng, X. Zhong, Y. Li, Q. Wang and D. Liu, *Cem. Concr. Compos.*, 2020, **110**, 103601.
51 H.-R. Jung, D.-H. Ju, W.-J. Lee, X. Zhang and R. Kotek, *Electrochim. Acta*, 2009, **54**, 3630–3637.
52 H. Wang, S. Zhang, M. Zhu, G. Sui and X. Yang, *J. Electroanal. Chem.*, 2018, **808**, 303–310.
53 W. Wang and A. Wang, *Appl. Clay Sci.*, 2016, **119**, 18–30.
54 H. Yin, M. Kong, X. Gu and H. Chen, *J. Cleaner Prod.*, 2017, **166**, 88–97.
55 H. Liu, T. Chen, D. Chang, D. Chen, C. Qing, J. Xie and R. L. Frost, *J. Therm. Anal. Calorim.*, 2012, **111**, 409–415.
56 Y. Zhang, C. Yu, P. Hu, W. Tong, F. Lv, P. K. Chu and H. Wang, *Appl. Clay Sci.*, 2016, **119**, 96–102.
57 Y. Zhang, L. Wang, F. Wang, J. Liang, S. Ran and J. Sun, *Appl. Clay Sci.*, 2017, **143**, 205–211.
58 A. A. Adeyemo, I. O. Adeoye and O. S. Bello, *Appl. Water Sci.*, 2017, **7**, 543–568.
59 A. Mishra, A. Mehta and S. Basu, *J. Environ. Chem. Eng.*, 2018, **6**, 6088–6107.
60 W. Jiang, Y. Jiang, S. Zhao, J. Peng, W. Qin, D. Ouyang and Y. Ding, *Energy Technol.*, 2019, **8**, 1901262.
61 M. Deka and A. Kumar, *Electrochim. Acta*, 2010, **55**, 1836–1842.
62 Y.-P. Wang, X.-H. Gao, R.-M. Wang, H.-G. Liu, C. Yang and Y.-B. Xiong, *React. Funct. Polym.*, 2008, **68**, 1170–1177.
63 J. Li, J. Yu, Y. Wang, J. Zhu and Z. Hu, *Ind. Eng. Chem. Res.*, 2020, **59**, 12879–12888.
64 X. Han, J. Yu, Z. Cao, R. Wang, W. Du, P. He and Y. Ge, *Constr. Build. Mater.*, 2020, **244**, 118408.
65 J. Liu, X. Cheng, Y. Zhang, X. Wang, Q. Zou and L. Fu, *Microporous Mesoporous Mater.*, 2017, **252**, 179–187.
66 P. Brea, J. A. Delgado, V. I. Águeda, P. Gutiérrez and M. A. Uguina, *Microporous Mesoporous Mater.*, 2019, **286**, 187–198.
67 A. Al-Ani, C. Freitas and V. Zholobenko, *Microporous Mesoporous Mater.*, 2020, **293**, 109805.
68 H. Wu, J. Lu, D. Xiao, Z. Yan, S. Li, T. Li, X. Wan, Z. Zhang, Y. Liu, G. Shen, S. Li and Q. Luo, *Food Hydrocolloids*, 2021, **110**, 106138.
69 J. Zhang, Q. Ping, M. Niu, H. Shi and N. Li, *Appl. Clay Sci.*, 2013, **83–84**, 12–16.
70 Z. Sun, S. Zheng, G. A. Ayoko, R. L. Frost and Y. Xi, *J. Hazard. Mater.*, 2013, **263**(Pt 2), 768–777.
71 L. Han, F. Li, H. Zhang, Y. Pei, L. Dong, F. Liang, Q. Jia and S. Zhang, *Adv. Appl. Ceram.*, 2020, **119**, 195–203.
72 韩雪, *塑料工业*, 2019, **47**, 24–27
73 N. Ediz, İ. Bentli and İ. Tatar, *Int. J. Miner. Process.*, 2010, **94**, 129–134.
74 F. Zhou, Z. Li, Y. Y. Lu, B. Shen, Y. Guan, X. X. Wang, Y. C. Yin, B. S. Zhu, L. L. Lu, Y. Ni, Y. Cui, H. B. Yao and S. H. Yu, *Nat. Commun.*, 2019, **10**, 2482.